APPLICATION OF THE MONTE CARLO METHOD IN THE SOLUTION OF RADIATION HEAT TRANSFER IN PARTICIPATING MEDIA

A. Maurente[a], P. O. Bayer[b], and F. H. R. França[c]

[a, b, c] Federal University of Rio Grande do Sul
Department of Mechanical Engineering
Rua Sarmento Leite, 425
90050-170, Porto Alegre
RS, Brazil
amaurente@mecanica.ufrgs.br
bpob@mecanica.ufrgs.br
cfrfranca@mecanica.ufrgs.br

ABSTRACT

The temperatures of the gases produced in combustion processes are very high so thermal radiation constitutes an important heat transfer mechanism in industrial furnaces. Most furnaces can be modeled as gray enclosures containing non-gray gases. The radiation heat transfer can be obtained with the aid of the weighted-sum-of-gray-gases model, determining the zonal exchange areas for each of the gray gases considered in the sum. For some enclosures with simple geometries, there are correlations to obtain the direct exchange-areas which can be used to determine the total exchange areas. However, for enclosures with complex geometries, determining the direct exchange areas can become a difficult task. In this case, the use of the Monte Carlo method is advantageous, for it allows one to approach geometric complexities without additional complications. Therefore, the method was applied to compute total exchange areas in enclosures containing participating media. Two cases were considered: cylindrical enclosures and enclosures that have generic geometries formed from cube combinations. The results presented a good agreement with solutions available in the literature.

Keywords: Radiative heat transfer, participating media, Monte Carlo method, zonal method

NOMENCLATURE

A	surface zone area, m^2.
L	cube edge, m.
E_b	blackbody emissive power, W/m^2.
f	frequency function.
G	gas zone in the total exchange-area (SG, GS or GG), m^2.
S	surface zone in the total exchange-area (SG, GS orSS), m^2.
I	total radiation intensity total, $W/m^2 \bullet sr$.
I_λ	spectral radiation intensity, $W/m^2 \bullet \mu m \bullet sr$.
K	total extinction coefficient, m^{-1}.
K_λ	spectral extinction coefficient, m^{-1}.
P	density probability function.
P_φ	emission angle of a energy package, rad.
P_r	emission radial location of a energy package, m.
P_x	x coordinate location of a energy package, m.
P_y	y coordinate location of a energy package, m.
P_z	z coordinate location of a energy package, m.
q	energy flux, W/m^2.
q_λ	spectral energy flux, $W/m^2\mu m$.
R	distribution cumulative function.
$Rand\beta$	random number related to β emission angle of a energy package.
$Rand\emptyset$	random number related to Ø emission angle of a energy package.
$Rand\varepsilon$	random number related to surface emissivity.
r_{max}	maximum value of radial coordinate in a zone, m.
r_{min}	minimum value of radial coordinate in a zone,
r_s	cylindrical surface of a cylindrical enclosure.
T	temperature, K.
V	volume, m^3.

Greek symbols

β	release polar angle of an energy package on the emission referential, rad.
$\beta_{ab,}$	release polar angle of an energy package on the absolute referential, rad.
ε	gray surface emissivity.
λ	wavelength of an energy package, μm.
ρ	gray surface refletivity.
Ø	release circumferential angle of an energy package on emission referential, rad.
$\emptyset_{ab}$	release circumferential angle of an energy package on absolute referential, rad.
φ	release angular position of an energy package, rad.
φ_{max}	maximum value of angular coordinate inside a zone, rad.
φ_{min}	minimum value of angular coordinate inside a zone, rad.
ω	solid angle, sr.

Superscripts

b	blackbody.
h	h zone (volume zone Gh with volume Vh).
i	incident.
i	i zone (surface zone Si with area Ai).
j	j zone (surface zone Sj with area Aj).
θ	angle (indicates angular dependence).
λ	wavelength (spectral dependence).

INTRODUCTION

There are several types of industrial furnaces. They are usually classified according to the fuel, which can be solid, liquid or gaseous. In furnaces that operate with gaseous fuel, the radiation fluxes have less importance than those that operate with liquid or solid fuels. Even so, because of the high temperature in which most of furnaces operate, the heteropolar gases, such as CO_2, H_2O, SO_2 and CO, emit and absorb energy so that the radiation heat transfer is of great importance.

In the calculations of radiation heat transfer, most of furnaces can be simulated as a gray enclosure containing non-gray gas. Generally, the zone method, first developed by Hottel and Sarofim (1967), can be applied in combination with the weighted-sum-of-gray-gases model. The major problems are determining the exchange areas between the zones and the gas properties. For a few simple enclosure geometries, it is available in the literature correlations to calculate the direct exchange-areas, which can be used to determine the total exchange-areas. Tucker (1986), using numerical integration, found correlations that can be used to calculate the direct exchange areas of cubic enclosures. Sika (1991) founded specific relations for cylindrical enclosures.

When the enclosure geometry is complex, the determination of exchange areas becomes more difficult. In this case, it is advantageous the use of the Monte Carlo method since this method makes it possible to approach geometry complexities without considerable additional difficulties.

In this work, the Monte Carlo method was applied to develop two algorithms that computes the total exchange-areas between zones in enclosures having participating media. The first algorithm determines total exchange-areas between gas and surfaces zones of a cylindrical enclosure. The enclosure can have any dimension and be divided into any number of zones with different extinction coefficients and surfaces emissivities. The second developed algorithm allows one to obtain total exchange-areas for enclosures with generic geometry formed by cube combinations.

THEORETICAL FOUNDATIONS

In order to apply the Monte Carlo method together with the zone method to calculate the total exchange-areas between zones of both types of enclosures, the following simplification was adopted: (1) all surfaces are gray and diffuse; (2) the gas is gray, (3) the gas does not scatter radiation so that the extinction coefficient is equal to the absorption coefficient; (4) each surface zone is small enough so that both the temperature and the emissivities are uniform in it; and (5) each gas zone is small enough so that both the temperature and the extinction coefficient is uniform in it.

CYLINDRICAL ENCLOSURES

For the case of cylindrical geometries, the enclosure dimension is defined by the height *H* and the radius *R*. The enclosure can be divided into any number of zones in both dimensions as well as in the angular position, as shown in Fig. 1 (a).

The emission location is determined in cylindrical coordinates referential shown in Fig. 1 (a), which will be called *geometry referential*. The emission and absorption angles of the packages are defined in a relative referential, which has its origin in the emission point. This referential will be called *emission referential*. Before determining both the angles and the emission location, they are transposed to the *path referential*, in Cartesian coordinates, shown in Fig. 1 (b).

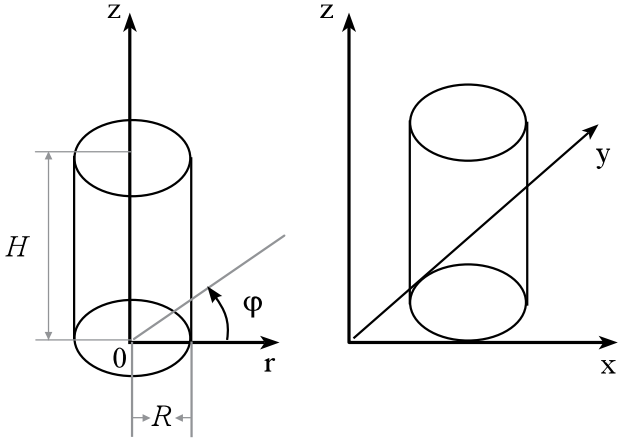

Figure 1. (a) Cylindrical enclosure defined in cylindrical coordinates and (b) Cartesian coordinates to follow the packages paths.

Because of the hypotheses (4) and (5), the emission probability of packages is the same anywhere in a given zone. The surface area of a zone belonging to the plane $z = 0$, $z = H$ or of any gas zone perpendicular section in the z direction is

$$A_Z = \frac{\Delta\varphi}{2} \cdot \left(r_{\max}^2 - r_{\min}^2\right) \tag{1}$$

where r_{min} and r_{max} are, respectively, the coordinates that limits the zones, and $\Delta\varphi$ is the increment φ angle. Therefore, considering total emission probability by this zone as 1.0, the emission probability from a infinitesimal area,

$$dA_Z = \Delta\varphi \cdot r \cdot dr, \tag{2}$$

within that zone where $r_{min} \le r \le r_{max}$, is

$$P = \frac{2 \cdot r \cdot dr}{\left(r_{\max}^2 - r_{\min}^2\right)} \tag{3}$$

The cumulative distribution function is

$$R = \int_{r_{\min}}^{r} \frac{2 \cdot r}{r_{\max}^2 - r_{\min}^2} dr = \frac{r^2 - r_{\min}^2}{r_{\max}^2 - r_{\min}^2} \tag{4}$$

Rewriting the above equation with R as a function of r and replacing R by $Randr$ and r by Pr (radial position), one obtains

$$P_r = \sqrt{Rand \cdot \left(r_{\max}^2 - r_{\min}^2\right) + r_{\min}^2} \tag{5}$$

where $Randr$ is a random number between 0 and 1.

The above equation gives the radial location of a released energy package.

The occurrence probability of a package emission is the same through both z and φ. Therefore, the angular and axial locations of the released packages are given, respectively, by

$$P_\varphi = \left(\varphi_{\max} - \varphi_{\min}\right) \cdot Rand \quad \varphi \tag{6}$$

and

$$P_Z = \left(z_{\max} - z_{\min}\right) \cdot Randz \tag{7}$$

where $Rand\varphi$ and $Randz$ are random numbers between 0 and 1.

As the surfaces are gray and diffuse, there is no preferential emission direction. Then, the package path angles can by determined by

$$\phi = 2\,\pi \cdot Rand\,\phi \tag{8}$$

and

$$\beta = \frac{\pi}{2} - arcsen\left(\sqrt{Rand\,\beta}\right) \tag{9}$$

where $Rand\beta$ and $Rand\phi$ are random numbers between 0 a 1. Both the β and ϕ angles are shown in Fig.. 2.

If the emission location and angles are known, it is possible to determine the package path from the release point to another surface point, if the package is not absorbed by the gas. The package path is a straight segment which can be found by its parametric equations:

$$\begin{cases} x = x_o + t \cdot \cos\beta_{ab} \cdot \cos\phi_{ab} \\ y = x_o + t \cdot \cos\beta_{ab} \cdot \cos\phi_{ab} \\ z = z_o + t \cdot \mathrm{sen}\beta_{ab} \end{cases} \tag{10}$$

where β_{ab} and ϕ_{ab} are, respectively, the β and ϕ release angles of the package rewritten in the path referential, x_o, y_o, and z_o are the coordinates on the emission point in the path referential, and t is the so-called *parameter* of the straight line. It is easy to verify that for each t value there is a corresponding point **P**. When t varies from $-\infty$ to $+\infty$, the **P** point describe the entire straight line. With both emission and angles locations in the absolute referential, it is possible to obtain the package path.

If the package is not absorbed by the gas during its travel, it reaches a surface zone. To determine this surface zone, it is necessary to find the intersection point between the straight line and the enclosures surfaces, that is, the $z = 0$ or $z = H$ planes or the $x^2+y^2=R^2$ cylindrical surface. The surface reached by the package is that in which the distance between the release and the intersection points is the smallest.

The participating gas also emits in the path referential. The release package angle ϕ_{ab} can be determined by Eq. (8). However, β_{ba} cannot be determined by Eq. (9), because surface emissions depend on the projected area in the emission direction. The equation for the gas emission angle β_{ba} is (according to Siegel, R. and Howell, J. R., 2002)

$$\beta_{ab} = \frac{\pi}{2} - \arccos\left(1 - 2 \cdot Rand\,\beta_{ab}\right) \tag{11}$$

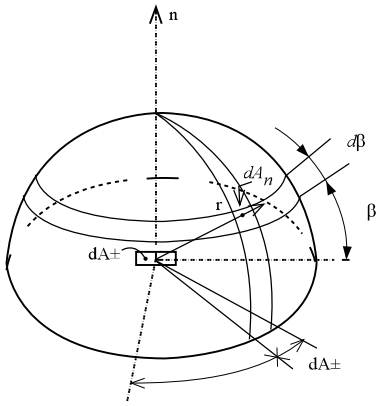

Figure 2. Emission angles of an energy package.

The path of a package emitted by the gas to a surface point, if it is not absorbed by the gas, can be determined in a similar way presented for packages emitted by surfaces.

To know if the package is absorbed by the gas, the Bouguer law can be employed, which states that

$$I_\lambda(S) = I_\lambda(0)\exp\left[\int_0^R K_\lambda(S^*)\cdot dS^*\right] \tag{12}$$

where S is the path length, S^* is a dummy variable of integration, $I_\lambda(0)$ is intensity of the radiation energy before crossing the media, and K_λ is the spectral absorption coefficient.

The fraction of radiation absorbed through a path of length $S+dS$ is

$$\frac{I_\lambda(S)-I_\lambda(S+dS)}{I_\lambda(0)} = \frac{-d\left[I_\lambda(S)/I_\lambda(0)\right]}{dS}dS = K_\lambda(S)\cdot\exp\left[\int_0^R K_\lambda(S^*)dS^*\right]dS \tag{13}$$

Since the gas is gray, the integration of the above equation through the wavelengths yields

$$\frac{-d\left[I(S)/I(0)\right]}{dS}dS = K\cdot e^{-K\cdot S}\cdot dS \tag{14}$$

The frequency function for this case is

$$f(S) = \frac{-d\left[I(S)/I(0)\right]}{dS} = K\cdot e^{-K\cdot S} \tag{15}$$

Therefore, the probability distribution function is

$$P(S) = \frac{e^{-K\cdot S}}{\int_0^\infty e^{-K\cdot S}dS} = K\cdot e^{-K\cdot S} \tag{16}$$

and the cumulative distribution function is

$$Rand(S) = \frac{\int_0^S e^{-K\cdot S}dS}{\int_0^\infty e^{-K\cdot S}dS} = 1-e^{-K\cdot S} \tag{17}$$

So, the path traveled by the package before being absorbed by gas is

$$S = \frac{1}{K}\ln(RandS) \tag{18}$$

where $RandS$ is a random number varying between 0 and 1.

If the gas properties are uniform throughout the package path, Equation (18) can be used to verify if the package is absorbed by the gas. In case it is absorbed, it must be obtained the position in the gas volume where it occurs. Then, the package energy is accounted for the zone in which the absorption occurs.

In case the gas properties are not uniform along the package travel, the path is divided into sections in which the gas properties can be consider uniform. So, Equation (18) can be used to verify if the package is absorbed in each path section.

When the package is not absorbed by the gas it reaches a surface. In that case, the probability that package is absorbed by the surface does not depend on the wavelength, for the surfaces are assumed as gray. The probability is then equal to the surface absorptivity (which is the same as the emissivity), so

$$Rand\varepsilon < \varepsilon \tag{19}$$

where ε is the surface emissivity and $Rand\varepsilon$ is a random number between 0 and 1. If $Rand\varepsilon < \varepsilon$, the package is absorbed, otherwise, it is reflected.

Every time a package is reflected, the reflection angles are determinate by Equations (8) and (9). Then the process above described is repeated again. The number of times that the reflections occur before the package is absorbed is not accounted; only the emitted and absorbed packages are accounted.

The above procedure should be repeated several times, that is, many energy packages must be emitted and accounted. The results will be the more accurate as the number of emitted packages is increased.

Enclosures Formed by Cube Combinations

In addition to cylindrical enclosures, the Monte Carlo method was applied to generate computer codes that can calculate exchange areas between zones of enclosures with generic geometries formed by cube combinations, each one being considered a single enclosure characterized by its side L.

The packages emission locations are obtained in the path referential, according to Figure 3. The emission angles are obtained in a relative referential whose origin is in the emission point (emission referential).

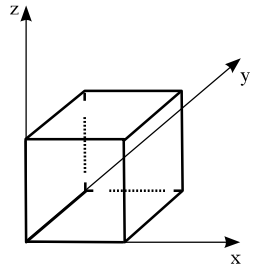

Figure 3. Cubic enclosure that constitute the generic geometric enclosures and the referential system of path.

From hypotheses 4 and 5 the emission probability of a package is the same anywhere in a given zone. Therefore, the emission location of a simulated package release can be found by the following relations:

$$Px = L \cdot Randx \tag{20}$$

$$Py = L \cdot Randy \tag{21}$$

$$Pz = L \cdot Randz \tag{22}$$

where Px, Py and Pz are, respectively, the release locations relatives to x, y and z and $Randx$, $Randy$ and $Randz$ are random numbers between 0 and 1.

The release angles can be found by Equations (8) and (9). The package path is obtained by Equation (10). If both the package path equation and the direction of the path are known, one can determine three among the six possible cube surfaces that cannot be reached by the package. To know which of remaining surface is reached by the package, it is necessary to find the intersection point between the path and the three remaining surfaces. It corresponds to the smallest path that the package needs to travel to reach a surface (unless the package is absorbed by gas before arriving at a surface).

When the packages are emitted by the gas, their emission angles can be calculated from Equations (8) and (11). The package path and the location where it is absorbed can be determined such as it is done for the packages emitted from a surface.

The absorption and reflection process for generic geometries are the same presented for those cylindrical ones. The major difference is that now the surfaces can be assigned as transparent, which allows the enclosure to be formed from other smaller (cubic) enclosures. When a package arrives at a transparent surface, instead of being absorbed or reflected it is transferred to the following cubic enclosure in the same position proceeding the same path.

RESULTS AND DISCUSSION

The two Monte Carlo codes were applied on solution of a few example problems. For some of this problems, applying techniques other than the Monte Carlo could became difficult. The results are presented in this section.

Results Obtained for Cylindrical Geometry

First, it was considered an enclosure similar to cylindrical furnaces, as tackled by Nunes and Naraghi, 1998. Its diameter and length are, respectively, 0.9 m and 5.0 m. The walls are diffuse and gray with emissivity of 0,8 and temperature of 450 K. The gas coefficient is 0.3 m^{-1}.

The enclosure was divided into 3×17 gas zones in order to consider all gas temperatures shown in Table 1. The surface zone number was assigned according to the gas zones so that there are three on the bottom, three on the top and seventeen on the lateral surfaces.

Table 1. Gas temperature field.

z, m	T(r=0,075m), K	T(r=0,225m), K	T(r=0,375m), K
0,15	1470	1120	870
0,45	1600	1320	1070
0,75	1620	1470	1360
1,05	1610	1550	1370
1,35	1580	1520	1350
1,65	1520	1470	1320
1,95	1470	1410	1280
2,25	1410	1360	1250
2,55	1350	1310	1210
2,85	1310	1260	1170
3,15	1270	1230	1150
3,45	1240	1200	1110
3,75	1200	1160	1090
4,05	1170	1130	1080
4,35	1140	1100	1070
4,65	1110	1080	1060
4,95	1080	1070	1060

The cylindrical surfaces heat flux can be found by

$$q_i = \frac{\left(\sum_{j=1}^{23} E_{s,j} \cdot S_j S_i + \sum_{h=24}^{74} E_h \cdot G_h S_i \right)}{A_i} - E_{s,i} \tag{23}$$

where S and G indicate surface and gas zones, respectively. The subscripts i, j refer to surface zones, h refers to the gas zones, so, for example, $S_j S_i$ is the total exchange area between the j and i surface zones; $G_h S_i$ is the total exchange area between h and i gas zones. The A_i is the surface area of i surface zone, $E_{b,h}$ is the blackbody emissive power of h gas zone and $E_{b,i}$ and $E_{b,i}$ are, respectively, the emissive power of i and j surface zones.

In Figure 4, it is shown the result for the radiation heat flux along the enclosure lateral surface. One result was calculated by the presented Monte Carlo algorithm while the other ones were obtained by Nunes and Naraghi, 1998.

The results presented above were obtained for a uniform gas coefficient for comparison with the results obtained by Nunes e Naraghi, 1998. However the developed Monte Carlo code can be applied to problems with non-

uniform gas properties as well. The non-uniform gas can be approached by Monte Carlo without much additional difficulties in comparison to uniform gas problems.

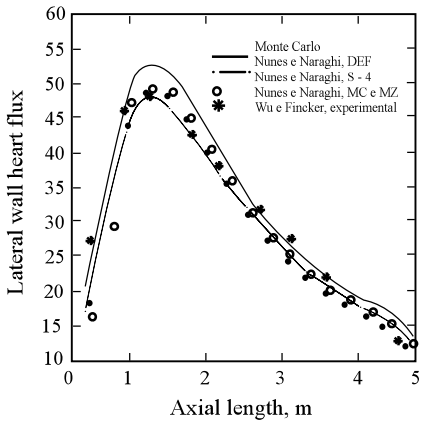

Figure 4. Radiation heat flux distribution in the lateral surface enclosure.

RESULTS FOR GENERIC GEOMETRIES FORMED BY CUBE COMBINATIONS

Next, total exchange-area results were obtained for two different geometries.

In the first case, it is considered a two-dimensional 1.0 m side enclosure with three baffles, as depicted in Figure 5.

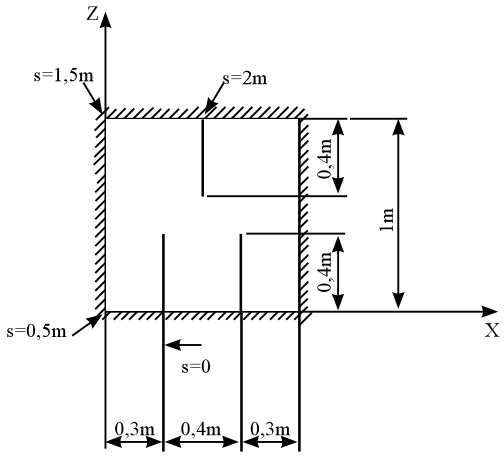

Figure 5. Geometry for the first case.

The emissive power and absorption coefficient the of gas are, respectively, 10 W/m^2 and 0,1 m^{-1}. The walls emissivity is 0.8 and the baffle emissivity is 0.6. The emissive powers of both the walls and the baffles is 1.0 W/m^2.

The *s* line shown in Figure 5, was divided into twenty surface zones and all gas forms only one single zone. The exchange-areas were first found, and next the heat flux in the *s* line (0-2 m) was computed using Equation (23).

Figure 6 shows the results obtained by the presented Monte Carlo algorithm as well as the results obtained for Coelho et al. (1998) using the discrete ordinate method (DTM).

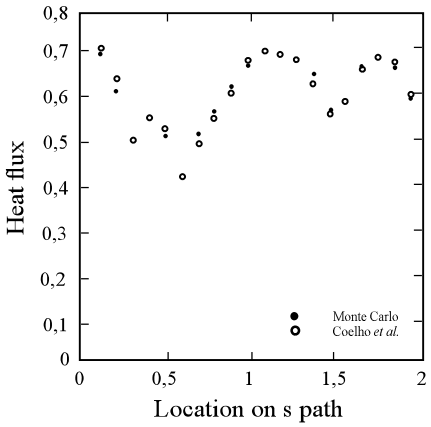

Figure 6. Radiation heat flux along *s*.

In the second case, it was found the heat fluxes in a three-dimensional enclosure similar to combustion chambers of some boilers. The enclosure geometry is shown in Figure 7. The baffles simulate super-heaters. The temperature and emissivities of the walls, including the baffle surfaces, were taken as 800 K and 0.65, respectively, except at x = 10 m and for 22 m $\leq z \leq$ 30 m, where the temperature was set equal 1200 K and the surface was assumed black. The extinction coefficients and temperatures of the participating media were set as the following: for z $\leq$ 5m, K= 0,2m^{-1} and T= 1600 K; for 5 m < $z \leq$ 10 m, K = 0,25 m^{-1} and T= 2000 K; for 10 m < $z \leq$ 20 m, K = 0,21 m^{-1} and T= 1600 K; and for 20 m < $z \leq$ 30 m, K = 0,181 m^{-1} and T= 1200 K.

The enclosure was modeled using several 0.2 m side cubes. The inclined walls were simulated in a stepwise fashion, according to Figure 8.

First, the total exchange-areas were found. For a better visualization of the results, Equation (23) was used to calculate the heat fluxes, which are shown for some enclosure surfaces in the following figures. The results obtained by the Monte Carlo method were compared with the results presented by Coelho et al. (1998). Figure 9 shows the heat flux in the surface in y = 0. In (a), it is shown the line of equal heat fluxes obtained by Coelho et al. (1998) from the discrete ordinates method. In (b) it is shown, in color map, the results obtained by the Monte Carlo method.

In Figure 9, for $z \geq 18$ m, the heat flux does not vary considerably, and the color scale used does not allow the visualization of the details, so Figure 10 shows the results only for $z \geq 18$ m, using another color scale.

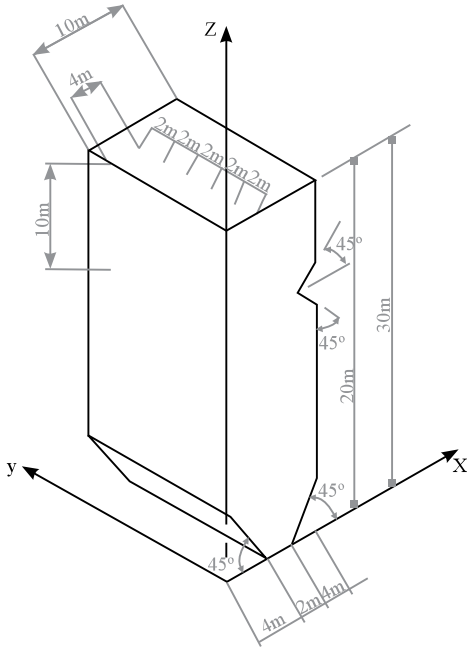

Figure 7. Enclosure for second case.

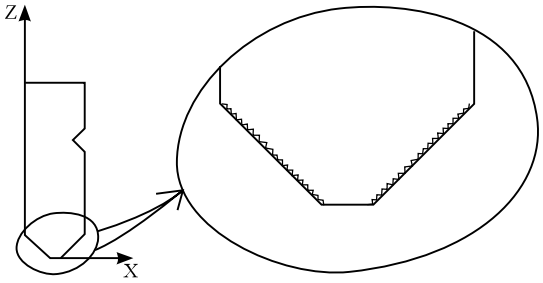

Figure 8. Modeling of inclined walls.

Inspecting Figures 9 and 10, it is noticed that the Monte Carlo results are not so smooth as those obtained for Coelho et al. (1998) . They are presented in color map since it would be difficult to visualize the lines of equal heat flux.

Many cubes were used to simulate the whole enclosure so the surface zones are rather small, having area of 0,04m^2. Therefore, only a few packages have been emitted or absorbed by them. This increased the statistical oscillations that is inherent of the Monte Carlo method. But the oscillations in the results were not significant for the computation of the heat transfer in the enclosure, since the heat fluxes in the larger regions were found summing the heat fluxes in the smaller surface zones (where the oscillations are more pronounced), a procedure that decreases the statistical oscillations.

Figure 11 also shows the results for $z \geq 18$ m but now the baffle are in a direction that is orthogonal to the figure plane. Figure 11 (a) refers to the $x = 0$ surface, and Figure 11 (b) refers to $x = 10$ m surface, which is located farther from the baffles. Observing Figure 11 (a), one notes that the heat flux is higher than 100 kW/m^2 up to $z = 20$ m, then it drops for the radiation flux is blocked by the baffles. The abrupt change in the heat flux that is seen in Figure 11 (b) is due to the fact that one of the inclined surfaces is turned to the hotter gas zone, while the other is turned to the colder gas zone.

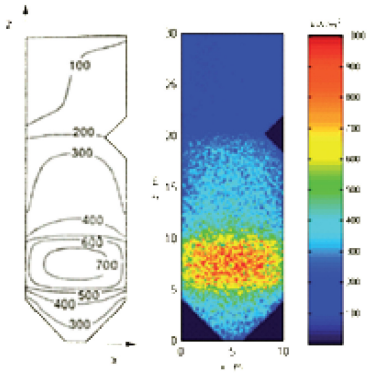

(a) (b)

Figure 9. Heat flux distribution in y=0. (a) Lines of equal heat flux [Coelho et al. (1998)]. (b) Color map, Monte Carlo.

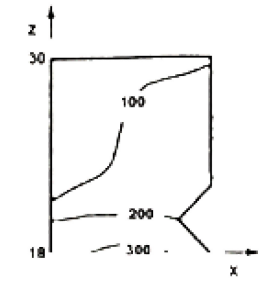

(a)

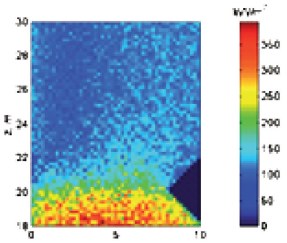

(b)

Figure 10. Heat flux for y=0 and $z \geq 18$m. (a) Lines of equal heat flux [Coelho et al. (1998)]. (b) Color map, Monte Carlo.

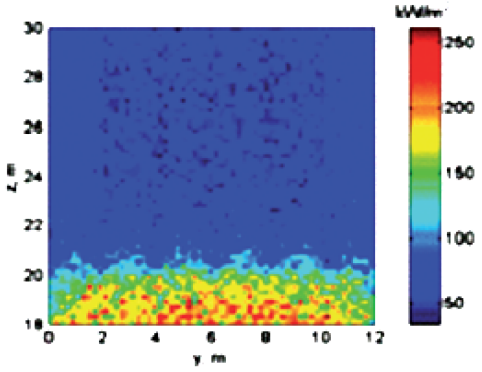

(a)

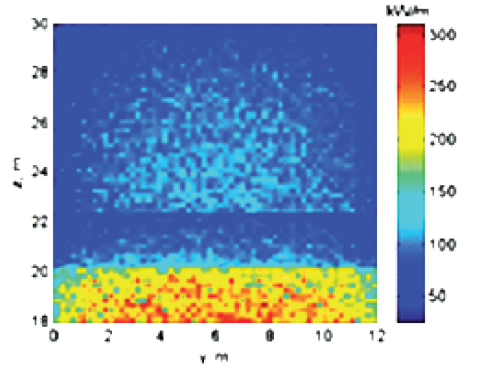

(b)

Figure 11. Heat flux for $z \geq 18$: (a) x=0, (b) $x \geq 10$ m.

CONCLUSIONS

When radiation heat flux in furnaces can be found by the weighted-sum-of-gray-gases model, which is a computation time saving method, it is advantageous to apply the Monte Carlo method together with the zone method to calculate the total exchange areas, especially when the enclosure is geometrically complex.

The Monte Carlo method was used to solve radiation heat transfer in participating media problems. Two type of geometries were considered: geometrically generic formed by cube combinations and cylindrical ones. By dealing with problems presenting enclosures with generic geometries, it was verified the capacity of the Monte Carlo method to approach geometrically complex systems.

The method flexibility was verified by showing that the same Monte Carlo computer codes was capable of solving problems, without additional difficulties, in which the properties, dimensions and even geometry were modified. Moreover, although the Monte Carlo was implemented without considering radiation scattering, based on the method characteristics, it can be stated that scattering could be easily implemented in computer codes, first including the scattering coefficient (*extinction coefficient = absorption coefficient + scattering coefficient*) and, secondly, determining the packages scattering probabilities.

ACKNOWLEDGEMENTS

This research was financially supported by CAPES-Brazil.

REFERENCES

Coelho P. J., Gonçalves, J. M. and Carvalho, M. G., 1998, Modelling of Radiative Heat Transfer in Enclosures with Obstacles, International Journal of Heat and Mass Transfer, Vol. 41, No. 4 – 5, pp. 745 – 756.

Hottel H. C. and Sarofim, A. F., 1967, Radiative Transfer, McGraw-Hill Book Company, New York. Howell, J. R., 1998, The Monte Carlo Method in Radiative Heat Transfer, Journal of Heat Transfer, vol. 120, no.3, pp. 547 – 560.

Modest, Michael F, 1991, The Weighted-Sum-of-Gray-Gases Model for Arbitrary Solution Methods in Radiative Transfer, Journal of Heat Transfer, Vol. 113, pp. 650 – 656. Nunes, E. M. and Naraghi, M. H. N., 1998, Numerical Model for Radiative Heat Transfer Analysis in Arbitrarily Shaped Gaseous Media, Numerical Heat Transfer, Part A, Vol. 33, No. 5, pp. 495 – 513.

Sika, J., 1991, Evalution of Direct Exchange Areas for a Cylindrical Enclosure, ASME J. Heat Transfer, Vol. 113, pp. 1040 – 1044.

Tucker, R. J., 1986, Direct Exchange Areas for Calculating Radiation Transfer in Rectangular Furnaces, Journal of Heat Transfer, Vol. 108, pp. 707 – 710.

Received: September 06, 2006
Revised: October 06, 2006
Accepted: November 06, 2006